Carbon Monoxide and Oxygen Binding to Human Hemoglobin F_0[†]

Enrico Di Cera,[‡,§] Michael L. Doyle,[‡] Marlo S. Morgan,[‡] Raimondo De Cristofaro,[∥] Raffaele Landolfi,[∥] Bruno Bizzi,[∥] Massimo Castagnola,[⊥] and Stanley J. Gill*[,‡]

Department of Chemistry and Biochemistry, University of Colorado, Boulder, Colorado 80309-0215, and Istituto di Semeiotica Medica and Istituto di Chimica, Università Cattolica, 00168 Roma, Italy

Received June 21, 1988; Revised Manuscript Received September 28, 1988

ABSTRACT: Differential binding curve measurements of carbon monoxide and oxygen binding to human hemoglobin F_0 under near-physiological conditions (0.1 M NaCl and 15 mM 2,3-diphosphoglyceric acid, pH 7.35, and 37 °C) have allowed a detailed description of the binding and linkage between these two gaseous ligands. Comparison with human hemoglobin A_0 under identical solution conditions shows that fetal hemoglobin F_0 binds oxygen and carbon monoxide with higher affinity than human hemoglobin A_0, but with the same cooperativity. Construction of the partition coefficient surface for carbon monoxide and oxygen binding reveals a failure of Haldane's laws for both hemoglobins. Linkage graphs are used to explore the phenomenological properties of the system. The graphs provide a quantitative description of the mechanism of carbon monoxide toxicity on oxygen transport by hemoglobin in vivo and demonstrate striking similarities between the functional properties of fetal and adult hemoglobins.

Fetal hemoglobin F_0 is the major O_2 carrier for the fetus and plays an important role in newborns until a few months after birth (Bunn & Forget, 1986). It is composed of two α chains identical with those of HbA_0[1] and two γ chains that differ from the β chains of HbA_0 in 39 residues (Schroeder et al., 1963). Notwithstanding its fundamental role in all stages of fetal development, little is known about the thermodynamic properties of HbF_0 under physiological conditions and how they compare with those of HbA_0. In this connection, the study of CO and O_2 binding to Hb at the heme site provides detailed information regarding the fundamental energetics involved. These ligands are "identically linked" in the sense defined by Wyman (1948), where either ligand, once bound to the heme, excludes the binding of the other. This feature greatly simplifies the analysis of the linkage and provides insights into the differences between the two ligands. We have recently found conditions that yield high-precision differential binding data for both ligands, either separately or in the presence of each other (Di Cera et al., 1987a). In the present study we apply the same experimental strategy to the analysis of CO and O_2 binding reactions to HbF_0 under near-physiological conditions and compare the results to those for HbA_0.

Materials and Methods

Experimental Conditions. Hemoglobin F_0 samples were prepared from umbilical cord blood. The cells were washed and lysed, and HbF_0 was separated on a column of Bio-Rex 70 (mesh 200–400) equilibrated against 0.050 M phosphate, pH 6.50, at 4 °C (Castagnola et al., 1983). The purity of the sample (>98% HbF_0) was tested by isoelectrofocusing of the globin chains (Castagnola et al., 1984). The samples were then concentrated under N_2, equilibrated against 0.1 M Hepes and 0.1 M NaCl, pH 7.40, and frozen in liquid N_2 until use. After thawing, the samples were reduced 4 h at 25 °C under an atmosphere of CO in the presence of an enzymatic reducing system (Hayashi et al., 1973). The final solution conditions were 1.2 mM heme, 0.1 m Hepes, 0.1 M NaCl, and 15 mM DPG, pH 7.36 at 37 °C, for HbF_0, and 2 mM heme, 0.1 M Hepes, 0.1 M NaCl, and 15 mM DPG, pH 7.35 at 37 °C, for HbA_0. All components of the enzymatic reducing system, the Hepes buffer, and DPG were products of Sigma Corp. The pH was precisely adjusted at 37 °C by a special gas-tight pH titration apparatus (Spokane et al., 1980). The temperature in the apparatus was controlled with a precision of ±0.01 °C from a water bath regulated by a Tronac, Inc., Model PTC-4 precision temperature controller.

Analysis of O_2 and CO binding to tetrameric Hb is facilitated by the use of highly concentrated Hb samples where dissociation into dimers is negligible. In a previous study we found that with a saturating amount of IHP (10 mM) a Hb concentration of 600 μM heme is high enough to neglect the effect of dimers (Di Cera et al., 1987a). This relatively low concentration further allowed us to measure the CO binding curve to the tetrameric form of Hb within a reasonably short time frame (<4 h). However, with the experimental conditions of the present study, we have found that, in order to neglect dissociation of Hb tetramers, a higher concentration was required. This suggests that IHP and DPG have different effects on the dimer–tetramer equilibrium.

Differential Binding Measurements. Differential binding curves were obtained with the thin-layer technique (Dolman & Gill, 1978). In this method the solution activity of the ligand is precisely defined at each point along the binding curve in terms of the partial pressure of the ligand in the gas phase. Initially, the Hb sample was equilibrated with O_2 at atmospheric pressure or CO at 2.5% of the atmospheric pressure. Changes in the ligand activity were then obtained by stepwise dilutions of the ligand partial pressure with N_2 gas, by means of a dilution valve connected to the gas-tight sample cell. The ligand partial pressure x_i after the ith stepwise dilution is given by

$$x_i = x_0 D^i \quad (1)$$

[†] This work was supported by NIH Grant HL22325.

[‡] University of Colorado.

[§] Present address: Istituto di Fisica, Università Cattolica, 00168 Roma, Italy.

[∥] Istituto di Semeiotica Medica, Università Cattolica.

[⊥] Istituto di Chimica, Università Cattolica.

[1] Abbreviations: Hb, hemoglobin; metHb, methemoglobin; Hepes, *N*-(2-hydroxyethyl)piperazine-*N*′-2-ethanesulfonic acid; IHP, inositol hexaphosphate; DPG, 2,3-diphosphoglyceric acid.

0006-2960/89/0428-2631$01.50/0

where x_0 is the initial partial pressure of the ligand and D is a constant dilution factor (in this study $D = 0.6972 \pm 0.0005$ for HbF_0 and 0.7031 ± 0.0006 for HbA_0). The path length of the Hb sample is determined by the thickness of the spacer shim used. In this study, due to the high affinity of CO and the high heme concentration required, we made especially thin stainless steel shims of thickness 7.5 μm (the shim stock was a gift from H. Cross Co.) to reduce equilibration time of CO with the sample solution to a practical value (3–20 min per step). Changes in the fractional saturation of either CO or O_2 were measured as changes in absorbance with a Cary 219 spectrophotometer in the Soret region. The percentage of metHb as measured by the ratio of absorbances at 578 and 500 nm in the spectrum of the fully oxygenated molecule was less than 2%.

The thin-layer method is intrinsically an equilibrium technique, as verified (1) by the constancy of the absorbance signal before and after each dilution step, (2) by its reversibility, and (3) by the high reproducibility of experimental results (Gill et al., 1987). For each stepwise dilution in the ligand partial pressure, the absorbance change is linearly related (Doyle et al., 1988) to the change in fractional saturation, so that

$$\Delta A(\xi_i) = \Delta A_T[\theta(x_i) - \theta(x_{i-1})] \quad (2)$$

Here θ is the fractional saturation of the macromolecule at a given ligand partial pressure, ΔA_T is the absorbance change on taking the macromolecule from zero to complete saturation, and ξ_i is the geometric mean, $(x_i x_{i-1})^{1/2}$, of the partial pressures defining the range of each step. The degree of saturation θ is equal to the number of ligand molecules bound per mole of Hb ($\bar{X}$ for O_2 or $\bar{Y}$ for CO) divided by 4, the number of binding sites. The change in absorbance at each step can be assigned to any value of x in the interval from x_i to x_{i-1}. In previous studies (Gill et al., 1987; Di Cera et al., 1987a) ΔA_i has been assigned to x_i. The choice of ξ_i is preferred here because the Taylor expansion of eq 2 gives with high precision (Di Cera & Gill, 1988)

$$\Delta A(\xi_i) = \Delta A_T\left(\frac{d\theta}{d \ln x}\right)_{\xi_i} = (\Delta A_T)(RT/4)\mathbf{B}(\xi_i) \quad (3)$$

This relation points out that the thin-layer method allows for direct measurement of the binding capacity $\mathbf{B}$[2] as a function of partial pressure. In the study of chemical binding phenomena, binding capacity measurements have the same significance as heat capacity measurements in the study of thermal transitions and thus reflect fundamental thermodynamic properties of the system (Di Cera et al., 1988).

Data Analysis. The overall equilibrium constant β_{ij} is defined by the reaction $M + iX + jY \rightarrow MX_iY_j$, where M denotes Hb, X is for O_2, and Y is for CO. These quantities, which determine the saturation function θ, and the optical parameter ΔA_T were estimated by least-squares minimization. All experimental points were weighted uniformly and analyzed in the form taken experimentally. In the fitting procedure none of the parameters were fixed to values that might be estimated independently. The absolute minimum of the χ^2 in the parameter space was searched and tested by different starting parameter guesses. Convergence was obtained in all cases to a unique set of best-fit parameter values. Reparametrization of the fitting problem in terms of the roots of the binding partition function yielded the same values of χ^2 and overall equilibrium constants in all cases. The roots have the unique advantage of being almost uncorrelated and thus drastically decrease the nonlinearity of the fitting procedure. They are calculated in any case to check the reliability of best-fit values obtained with other parameterizations where correlation may be high. Parameter errors were estimated by F tests at the cutoff of one standard deviation (67% confidence). Hewlett-Packard 9816 and 9000/300 computers were employed for all analyses.

[2] The symbol $\mathbf{B}$ (Caslon open font) is used in this paper in place of the Russian B chosen in the original definition (Di Cera et al., 1988), since the Russian B is not one of the characters available to this Journal.

Table I: Overall Equilibrium Constants (β_{ij}),[a] Median Partial Pressures (p_m), and Partition Coefficients (m_i) for O_2 and CO Binding to HbF_0 and HbA_0

O_2 binding parameters	CO binding parameters
HbF_0	
$\beta_{10} = 0.085$ (0.074, 0.098)[b] $Torr^{-1}$	$\beta_{01} = 6.28$ (5.61, 7.30) $Torr^{-1}$
$\beta_{20} = 0.0019$ (0.0016, 0.002) $Torr^{-2}$	$\beta_{02} = 86.2$ (73.3, 95.0) $Torr^{-2}$
$\beta_{30} = 0$ (5.3×10^{-6}) $Torr^{-3}$	$\beta_{03} = 0$ (22) $Torr^{-3}$
$\beta_{40} = 8.2 \times 10^{-6}$ (7.4×10^{-6}, 9.0×10^{-6}) $Torr^{-4}$	$\beta_{04} = 1.1 \times 10^4$ (9880, 1.2×10^4) $Torr^{-4}$
$p_m = 18.7$ (18.2, 19.2) Torr	$p_m = 0.098$ (0.095, 0.10) Torr
ΔA_T[c] = 0.3219 (0.3195, 0.3251)	$\Delta A_T = 0.0967$ (0.0956, 0.0975)
σ[c] = 0.00058	$\sigma = 0.00010$
m_1[d] $= \beta_{01}/\beta_{10} = 74$ (57, 99)	$m_2 = (\beta_{02}/\beta_{20})^{0.5} = 213$ (191, 244)
$m_4 = (\beta_{04}/\beta_{40})^{0.25} = 191$ (182, 201)	
HbA_0	
$\beta_{10} = 0.049$ (0.043, 0.053) $Torr^{-1}$	$\beta_{01} = 3.98$ (3.41, 4.19) $Torr^{-1}$
$\beta_{20} = 0.00094$ (0.00090, 0.0010) $Torr^{-2}$	$\beta_{02} = 40.8$ (37.6, 43.2) $Torr^{-2}$
$\beta_{30} = 0$ (5.1×10^{-7}) $Torr^{-3}$	$\beta_{03} = 0$ (21) $Torr^{-3}$
$\beta_{40} = 1.7 \times 10^{-6}$ (1.5×10^{-6}, 1.9×10^{-6}) $Torr^{-4}$	$\beta_{04} = 2766$ (2504, 2942) $Torr^{-4}$
$p_m = 27.7$ (26.9, 28.6) Torr	$p_m = 0.14$ (0.13, 0.15) Torr
$\Delta A_T = 0.0436$ (0.0412, 0.0478)	$\Delta A_T = 0.0900$ (0.0821, 0.0976)
$\sigma = 0.00011$	$\sigma = 0.00020$
$m_1 = \beta_{01}/\beta_{10} = 81$ (64, 97)	$m_2 = (\beta_{02}/\beta_{20})^{0.5} = 208$ (219, 194)
$m_4 = (\beta_{04}/\beta_{40})^{0.25} = 201$ (190, 210)	

[a] β_{ij} is defined for the reaction $Hb + iO_2 + jCO \rightarrow Hb(O_2)_i(CO)_j$. [b] Values shown in parentheses represent 67% confidence upper and lower limits. [c] Fitted value absorbance change; σ is standard error of fitted absorbance values. [d] Partition coefficient ratios, m_i, for reactions $(1/i)Hb(O_2)_i + CO = (1/i)Hb(CO)_i + O_2$.

Results

O_2 and CO Binding Curves. The CO and O_2 binding curves of HbF_0 and HbA_0 were measured under identical solution conditions and the results for HbF_0 are shown in Figure 1a,b as differential, or binding capacity, data. The analysis of the O_2 binding data, in the absence of CO, yields the values for the overall O_2 equilibrium constants β_{10}, β_{20}, β_{30}, and β_{40}. Likewise the CO equilibrium constants β_{01}, β_{02}, β_{03}, and β_{04} are determined from the CO binding curve, in the absence of O_2. From Table I one sees that HbF_0 has a higher affinity than HbA_0 for both O_2 and CO. As found in recent studies (Gill et al., 1987; Di Cera et al., 1987a), we observe negligible values of β_{30} and β_{03} for both hemoglobins. This result points out that, although some structural differences do exist between HbA_0 and HbF_0 (Frier & Perutz, 1977), the energetic features of reactions for O_2 and CO binding to these two hemoglobins are similar. This similarity is also seen in Figure 2 in the comparable distribution of intermediates for O_2 and CO binding. However the plot of the binding capacity of the two ligands, shown in Figure 3, clearly reveals a substantial difference in the shape of the two binding curves, especially at low saturation, for both HbF_0 and HbA_0. This observation agrees with the results obtained with IHP (Di Cera et al., 1987a). A quantitative measure of the difference in O_2 and CO binding is revealed by the partition coefficient m_i defined

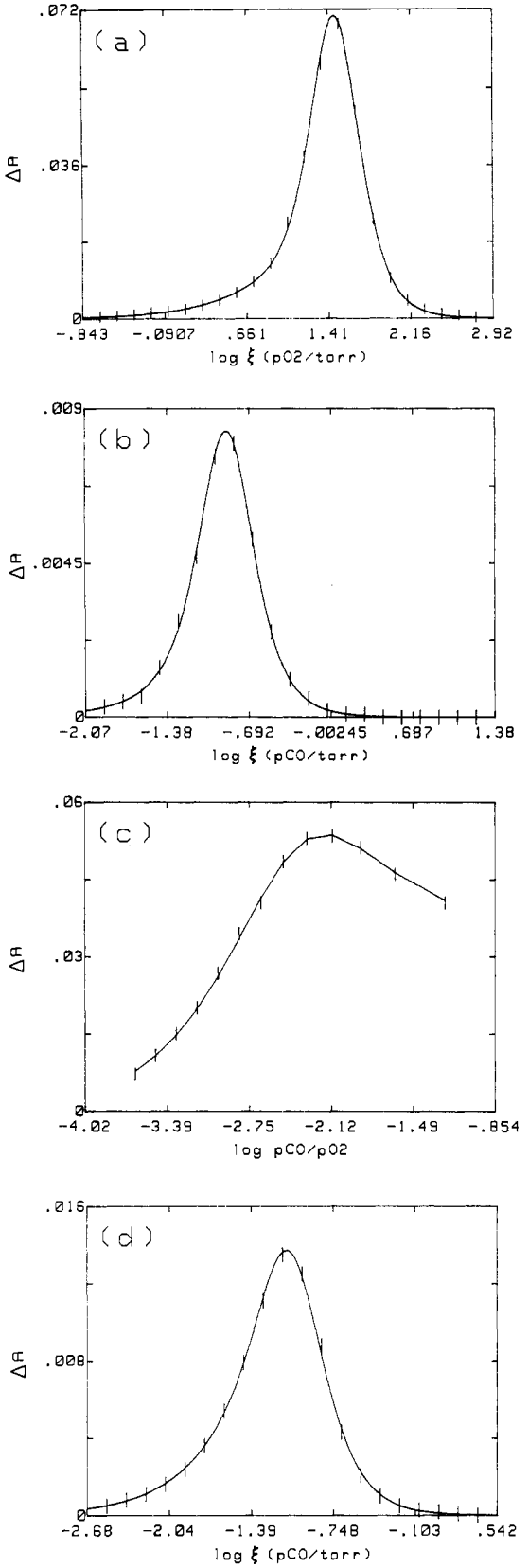

FIGURE 1: Differential measurements of O_2 and CO binding to HbF_0 in the experimental conditions described in the text. The data were obtained as changes in absorbance upon stepwise dilutions of the ligand partial pressure by means of the thin-layer method. The value ξ is equal to the geometric mean of the initial and final partial pressures at each dilution step. Vertical bars are four times the standard error of the fit. The best-fit parameter values obtained from analysis of the experiments are listed in Tables I and II. (a) O_2 binding curve; (b) CO binding curve; (c) O_2–CO competition experiment; (d) constant ratio experiment.

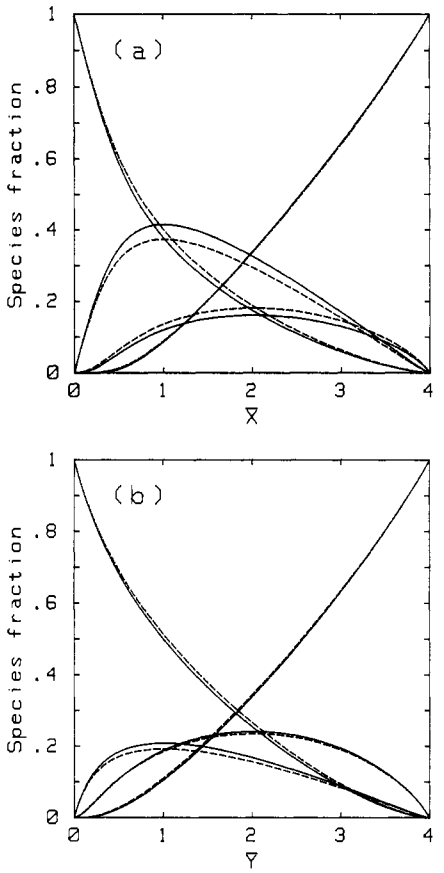

FIGURE 2: Ligated species fractions of stoichiometric intermediates for O_2 (a) and CO (b) as a function of the moles of ligand bound per mole of macromolecule, using the best-fit values of the β's summarized in Table I: (continuous line) HbF_0; (dotted line) HbA_0.

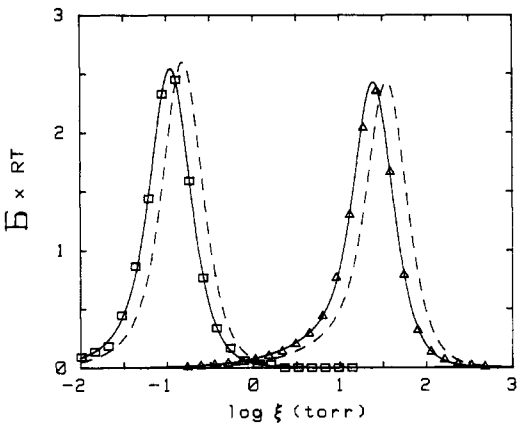

FIGURE 3: O_2 (△) and CO (□) binding capacity [$B = (1/RT)(\partial \bar{X} / \partial \ln x)_{\ln y}$] of HbF_0 in the experimental conditions described in the text. The data obtained as shown in Figure 1a,b were transformed according to eq 3 to match the binding capacity curves drawn with the best-fit parameter values reported in Table I. The O_2 and CO binding capacities of HbA_0 under identical solution conditions are shown by dotted lines.

for the stoichiometric replacement $MX_i + iY \rightarrow MY_i + iX$, normalized by the number of ligands i (see Table I). The ratio of the median partial pressure (Wyman, 1964) for O_2 and CO gives the partition coefficient m_4 for the fully ligated molecule. The value obtained is 191 for HbF_0, and 201 for HbA_0, in essential agreement with previous work (Roughton, 1970). With the values of the other overall Adair constants for both O_2 and CO, one can calculate the values of m_1 and m_2, corresponding to the singly and doubly ligated molecule. The value of m_1 is significantly different from m_4 for both HbF_0

Table II: Binding Parameters for the Competition and Constant Ratio Experiments

competition experiment[a]	constant ratio experiment[b]
HbF_0	
C_1 = 724 (652, 802)[c]	E_1 = 27.3 (24.6, 31.4) $Torr^{-1}$
$C_2 = 1.9 \times 10^5$ (1.6×10^5, 2.1×10^5)	E_2 = 753 (626, 834) $Torr^{-2}$
$C_3 = 2.5 \times 10^7$ (2.1×10^7, 2.8×10^7)	E_3 = 0 (25.3) $Torr^{-3}$
$C_4 = 1.1 \times 10^9$ (1.0×10^9, 1.3×10^9)	$E_4 = 1.9 \times 10^5$ (1.7×10^5, 2.2×10^5) $Torr^{-4}$
ΔA_T = 0.4665 (0.4620, 0.4715)	ΔA_T = 0.0790 (0.0782, 0.0799)
σ = 0.00053	σ = 0.00018
HbA_0	
C_1 = 847 (753, 932)	E_1 = 17.7 (16.0, 20.2) $Torr^{-1}$
$C_2 = 2.2 \times 10^5$ (1.9×10^5, 2.5×10^5)	E_2 = 280 (235, 309) $Torr^{-2}$
$C_3 = 2.9 \times 10^7$ (2.5×10^7, 3.3×10^7)	E_3 = 0 (35.6) $Torr^{-3}$
$C_4 = 1.4 \times 10^9$ (1.3×10^9, 1.6×10^9)	$E_4 = 4.7 \times 10^4$ (4.3×10^4, 5.0×10^4) $Torr^{-4}$
ΔA_T = 0.1440 (0.1426, 0.1454)	ΔA_T = 0.0367 (0.0363, 0.0371)
σ = 0.00024	σ = 0.000064

[a] Parameters C_i are equal to $\beta_{4-i,i}/\beta_{40}$ representing the reactions $Hb(O_2)_4 + iCO = Hb(O_2)_{4-i}(CO)_i + iO_2$. [b] Parameters E_i are defined in the text following eq 10. [c] Values shown in parentheses represent 67% confidence upper and lower limits.

and HbA_0, indicating a failure of Haldane's laws (Haldane & Smith, 1897).

O_2–CO Competition Experiment. The equilibria among the fully ligated species MX_4, MX_3Y, MX_2Y_2, MXY_3, and MY_4 can be determined by saturating the molecule with one ligand and measuring its replacement through a series of increasing relative activities of the other ligand (Wyman et al., 1982; Di Cera et al., 1987a). In this experiment Hb was saturated with CO at 2.5% P_a (P_a = atmospheric pressure − vapor pressure of H_2O), followed by dilution with O_2 at pressure P_a. At each dilution step the CO partial pressure is

$$y_i = y_0 D^i = 0.025 P_a D^i \quad (4)$$

and the O_2 partial pressure is

$$x_i = x_0(1 - D^i) = P_a(1 - D^i) \quad (5)$$

It is convenient to write the binding partition function (see Appendix for details) for this experiment in terms of the fully ligated species by taking MX_4 as the reference species, so that

$$\Xi(x,y) = \frac{\beta_{40}x^4 + \beta_{31}x^3y + \beta_{22}x^2y^2 + \beta_{13}xy^3 + \beta_{04}y^4}{\beta_{40}x^4} \quad (6)$$

Upon rearrangement eq 6 becomes

$$\Xi(z) = 1 + C_1 z + C_2 z^2 + C_3 z^3 + C_4 z^4 \quad (7)$$

where $C_1 = \beta_{31}/\beta_{40}$, $C_2 = \beta_{22}/\beta_{40}$, $C_3 = \beta_{13}/\beta_{40}$, $C_4 = \beta_{04}/\beta_{40}$, and $z = y/x$. The differential measurements are shown in Figure 1c. Analysis of the data according to the finite-difference fitting equation (2) yields the C's summarized in Table II. For both hemoglobins these constants are statistical, demonstrating that all the fully ligated states from MX_4 to MY_4 are distributed as expected for a noncooperative system. This implies that the O_2–CO replacement reaction occurs at each site independently (Wyman et al., 1982; Di Cera et al., 1987a).

The Constant Ratio Experiment. In this experiment Hb is saturated with a gas mixture of O_2 and CO produced with $0.025P_a$ of CO and then diluted with pure O_2 by using the thin-layer dilution valve. After five dilutions all the fully ligated species were populated. The gas mixture was then diluted with N_2 so that all the intermediates, in any possible combination of CO and O_2, were progressively populated, eventually leading to the unligated form. The fitting equation for this experiment is

$$\Delta A(\xi_i) = \Delta A_{TY}[\bar{Y}(x_i) - \bar{Y}(x_{i-1})]/4 + \Delta A_{TX}[\bar{X}(x_i) - \bar{X}(x_{i-1})]/4 \quad (8)$$

Here the different spectral contributions of HbCO (ΔA_{TY}) and HbO_2 (ΔA_{TX}) must be taken into account. Measurements at the isosbestic point for HbCO and HbO_2 (where $\Delta A_{TY} = \Delta A_{TX} = \Delta A_T$) simplify eq 8 to

$$\Delta A(\xi_i) = \Delta A_T[\bar{T}(x_i) - \bar{T}(x_{i-1})]/4 \quad (9)$$

The ratio $\rho = x/y$ (see Table II) remains unchanged in this experiment, and therefore the total saturation is given by

$$\bar{T} = \frac{E_1 y + 2E_2 y^2 + 3E_3 y^3 + 4E_4 y^4}{1 + E_1 y + E_2 y^2 + E_3 y^3 + E_4 y^4} \quad (10)$$

where $E_1 = \beta_{10}\rho + \beta_{01}$, $E_2 = \beta_{20}\rho^2 + \beta_{11}\rho + \beta_{02}$, $E_3 = \beta_{30}\rho^3 + \beta_{21}\rho^2 + \beta_{12}\rho + \beta_{03}$, and $E_4 = \beta_{40}\rho^4 + \beta_{31}\rho^3 + \beta_{22}\rho^2 + \beta_{13}\rho + \beta_{04}$. The data are shown in Figure 1d. They are a measure of the change in the total saturation $\bar{T} = \bar{X} + \bar{Y}$ due to a change in the O_2 and CO chemical potential, μ_X and μ_Y, such that the difference $\mu_Y - \mu_X$ is constant. This is because the ratio x/y is constant at any dilution and the partial pressures of both gases decrease by the same amount. Analysis of the results is summarized in Table II. The best-fit value of E_3 is zero for both HbA_0 and HbF_0, demonstrating that all the triply ligated species, in any combination of O_2 and CO, are negligible. The proportions of fully ligated species in this experiment are in good agreement with those observed in the competition experiment, and the equilibrium constants for the singly and doubly ligated species match those found in separate CO and O_2 binding curves.

Simultaneous Data Analysis. The four types of experiments described above must form a self-consistent thermodynamic cycle, where the values of the overall equilibrium constants β determined in different experiments are the same (Di Cera et al., 1987a). In a simultaneous fit of all the data possible inconsistencies would be revealed. The best-fit values of the β's obtained in the simultaneous fit are listed in Table III and are in excellent agreement with the values determined in the separate fits. The parameter ρ, equal to the ratio x/y in the constant ratio experiment, was floated in the simultaneous fit, and a value identical with that expected for five dilution steps was obtained for both HbA_0 and HbF_0. All parameters entering the fitting equation for each experiment were floated. Different starting guesses were given, and the same minimum was reached in all cases.

As is to be noted in Table III, the best-fit equilibrium constants for forming any of the triply ligated species are found to be negligibly small. Other high-precision studies of oxygen binding (Mills et al., 1976; Chu et al., 1984) allow within indicated error estimates for the values we find using the thin-layer technique. We feel that the derivative measurements obtained by the thin-layer method provide data of higher precision than can be obtained by the alternative scanning approach, which relies upon measurements of total optical changes as a function of oxygen concentration determined with an oxygen electrode. The thin-layer method also allows use of high hemoglobin concentrations, which simplifies the data analysis to tetrameric species alone. Moreover, the different formulation of appropriate equations for analysis of data obtained in the respective methods leads to a fundamental difference in the nonlinear problem defining the parameters of the system. Ratkowsky (1983) has discussed general aspects of this problem regarding the influence of specific formulations

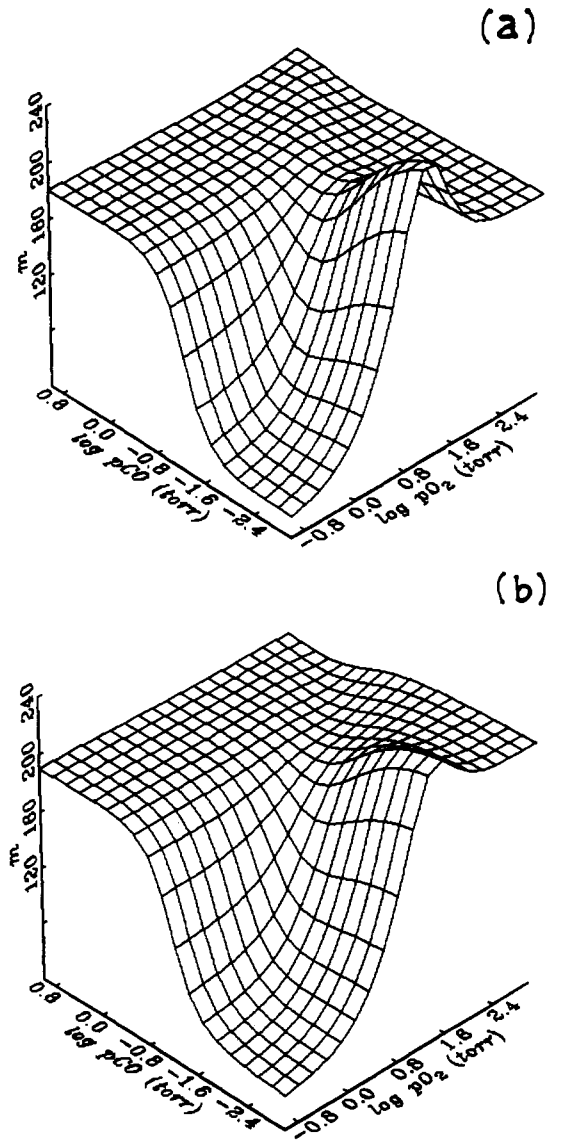

FIGURE 4: Partition coefficient [$m = (\bar{Y}/\bar{X})(x/y)$] surfaces for CO and O_2 binding to HbF_0 (a) and HbA_0 (b) as a function of CO and O_2 partial pressures. The surfaces were constructed according to eq A8 with the values of the overall equilibrium constants β listed in Table III.

upon the bias of error estimates. Simulation studies (Gill et al., 1988) show (1) that the formulation used in the analysis of the thin-layer results leads to near-Gaussian error distributions and (2) that fixing a parameter in the fitting equation can have a strong influence on the values determined for other parameters. These effects might account for the small differences found between the various high-precision studies.

Discussion

This study provides a self-consistent set of data for the O_2 and CO binding reactions to HbF_0 and HbA_0 and allows for quantitative conclusions on the identical linkage between these ligands under physiological conditions. We first find that the shape of the O_2 binding curve for both Hbs is different from that of CO and thus that Haldane's laws do not hold. Second, the partition coefficient surface for HbF_0, shown in Figure 4a, is practically identical with that of HbA_0 (Figure 4b). One sees how the surface changes drastically in going from low to high values of x and y. Only at high saturation is it flat, thus implying the validity of Haldane's laws in this region (Wyman et al., 1972; Di Cera et al., 1987a). The thermodynamic basis

Table III: Equilibrium Parameters Determined by a Simultaneous Fit of All the Four Experiments Discussed in the Text [Pure O_2 Binding, Pure CO Binding, Competitive Binding, and Dilution at a Fixed Ratio (ρ)[a] of O_2 and CO Partial Pressures]

HbF_0	
β_{10}[b] = 0.088 ± 0.012[c] $Torr^{-1}$	β_{04} = 9458 ± 72.5 $Torr^{-4}$
β_{20} = 0.0019 ± 0.00015 $Torr^{-2}$	β_{31} = 0.0060 ± 0.00081 $Torr^{-4}$
β_{30} = 0 ± 4.1 × 10^{-7} $Torr^{-3}$	β_{22} = 1.62 ± 0.07 $Torr^{-4}$
β_{40} = 8.3 × 10^{-6} ± 1.1 × 10^{-6} $Torr^{-4}$	β_{13} = 209 ± 13 $Torr^{-4}$
β_{01} = 5.32 ± 0.88 $Torr^{-1}$	β_{21} = 0 ± 6.9 × 10^{-4} $Torr^{-3}$
β_{02} = 76.2 ± 6.6 $Torr^{-2}$	β_{12} = 0 ± 0.12 $Torr^{-3}$
β_{03} = 0 ± 47 $Torr^{-3}$	β_{11} = 2.93 ± 0.11 $Torr^{-2}$
σ[d] = 0.00040	$\rho = p_0(O_2)/p_0(CO)$ 203 ± 7
m_1[e] = β_{01}/β_{10} = 60 ± 11	$m_2 = (\beta_{02}/\beta_{20})^{0.5}$ = 200 ± 23
$m_4 = (\beta_{04}/\beta_{40})^{0.25}$ = 184 ± 24	
HbA_0	
β_{10} = 0.051 ± 0.002 $Torr^{-1}$	β_{04} = 2734 ± 22.7 $Torr^{-4}$
β_{20} = 0.00099 ± 0.00008 $Torr^{-2}$	β_{31} = 0.0016 ± 0.00021 $Torr^{-4}$
β_{30} = 0 ± 9.1 × 10^{-6} $Torr^{-3}$	β_{22} = 0.43 ± 0.02 $Torr^{-4}$
β_{40} = 1.8 × 10^{-6} ± 1.1 × 10^{-7} $Torr^{-4}$	β_{13} = 57.4 ± 3.2 $Torr^{-4}$
β_{01} = 3.89 ± 0.24 $Torr^{-1}$	β_{21} = 0 ± 2.0 × 10^{-4} $Torr^{-3}$
β_{02} = 40.5 ± 3.2 $Torr^{-2}$	β_{12} = 0 ± 0.06 $Torr^{-3}$
β_{03} = 0 ± 10 $Torr^{-3}$	β_{11} = 1.04 ± 0.06 $Torr^{-2}$
σ = 0.00016	$\rho = p_0(O_2)/p_0(CO)$ = 185 ± 9
$m_1 = \beta_{01}/\beta_{10}$ = 76 ± 6	$m_2 = (\beta_{02}/\beta_{20})^{0.5}$ = 202 ± 23
$m_4 = (\beta_{04}/\beta_{40})^{0.25}$ = 197 ± 12	

[a] ρ is equal to the ratio of the O_2/CO partial pressures, which remains constant during the experiment. [b] β_{ij} is defined for the reaction $Hb + iO_2 + jCO \rightarrow Hb(O_2)_i(CO)_j$. [c] The errors on the parameters are equal to twice the error estimates provided in the nonlinear least-squares minimization procedure. [d] σ is the standard error of the fitted absorbance values. [e] Partition coefficient ratios, m_i, for reactions $(1/i)Hb(O_2)_i + CO = (1/i)Hb(CO)_i + O_2$.

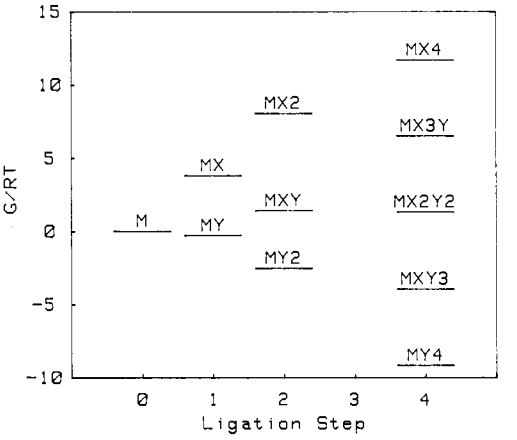

FIGURE 5: Free energy levels for the identical linkage of CO (y) and O_2 (x) to HbF_0 calculated from the overall equilibrium constants listed in Table III. The constants were all corrected for statistical factors to allow comparison of all levels in terms of intrinsic free energy changes. The statistical factors g_{ij} for the overall equilibrium constants β_{ij} are $4!/i!j!(4-i-j)!$, and the levels shown are equal to $-\ln(\beta_{ij}/g_{ij})$. The reference species M has been assigned the same energy level of the standard state corresponding to 1 Torr in the gas phase, and the other levels were calculated accordingly. The manifold of the triply ligated species cannot be located due to their negligible contribution to the ligation process.

for the failure of Haldane's laws is revealed by the statistically corrected energy levels for the identical linkage between O_2 and CO. These levels are shown in Figure 5 for HbF_0. The mixed doubly ligated species MXY is more populated than expected by a statistical distribution with respect to MX_2 and MY_2, so that the energy level of MXY is not equal to the average of the energy levels of MX_2 and MY_2. Consequently, cooperativity must exist in the CO–O_2 replacement reaction for the doubly ligated molecule, unlike the case of the fully

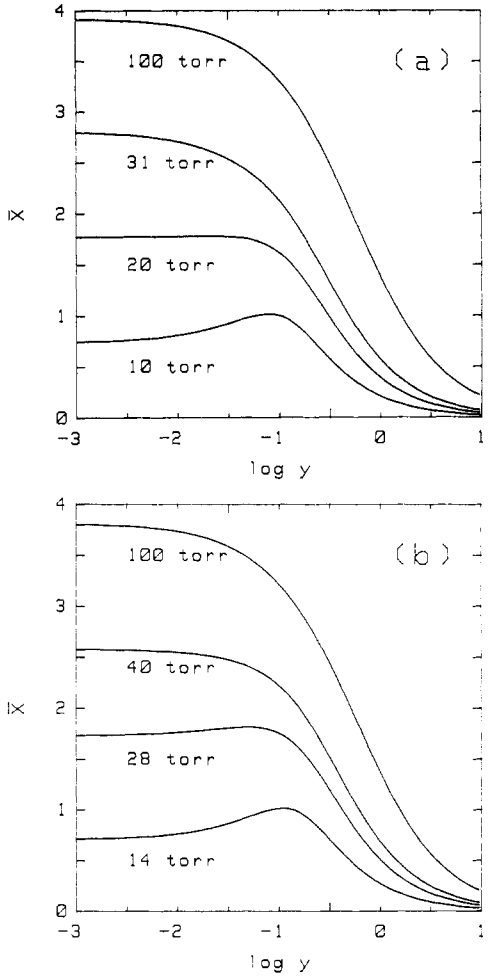

FIGURE 6: Linkage graph of the number of oxygens bound, $\bar{X}$, as a function of the CO partial pressure, y, at the indicated constant values of the O_2 partial pressure x: (a) HbF_0; (b) HbA_0.

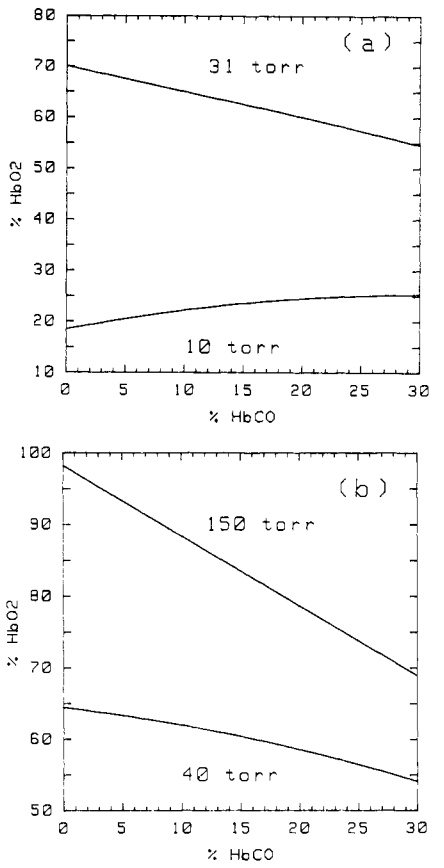

FIGURE 7: Linkage graph of the number of oxygens bound, $\bar{X}$, versus the number of carbon monoxides bound, $\bar{Y}$, at constant value of the O_2 partial pressure x as indicated. The difference between the two curves yields the arteriovenous gradient for O_2 transport from the placenta to tissues in the case of HbF_0 (a) and from lungs to tissues in the case of HbA_0 (b).

ligated molecule. The energetic levels of the fully ligated species, in fact, are equally spaced. This explains why the CO and O_2 binding curves are not parallel at low saturation, which leads to a failure of Haldane's laws. The same conclusion holds for HbA_0.

The choice of the particular experimental conditions used in this study allows one to assess some features of the identical linkage between O_2 and CO of possible physiological relevance. These features are readily displayed by linkage graphs (Wyman, 1984) constructed from the partition function (see Appendix for details). The first graph shows the number of oxygens bound, $\bar{X}$, as a function of y, the CO partial pressure, when the O_2 partial pressure x is constant (see Figure 6). One observes that an increase of y reduces $\bar{X}$ as expected; however, for low values of x an increase of y leads "paradoxically" to an increase of $\bar{X}$. In this domain CO promotes O_2 binding. As a consequence of the linkage relation eq A5a, there exists a domain of y where O_2 promotes CO binding. This effect in a less comprehensive form was observed by Haldane 76 years ago on whole blood (Douglas et al., 1912) and is a consequence of the cooperative nature of the O_2 and CO binding curves. The second linkage graph depicts the number of oxygens bound, $\bar{X}$, as a function of the number of carbon monoxides bound, $\bar{Y}$, while keeping x constant (see Figure 7). In the case of HbA_0 the upper curve is calculated for $x = 150$ Torr, the value of O_2 partial pressure in the lungs, and the lower curve for $x = 40$ Torr, the value of O_2 partial pressure in the tissues. One sees how the toxicity of CO (i.e., the decreasing difference between these curves) is due to a progressive decrease of the arteriovenous gradient for O_2 transport from lungs to tissues. In the case of HbF_0 the two different O_2 partial pressures correspond to the umbilical vein (31 Torr) and the umbilical artery (10 Torr) (Dawes, 1976). Figure 7a shows that HbF_0 functions in vivo over a wider saturation range than HbA_0, which results in a greater amount of O_2 being unloaded to the tissues. Furthermore, the "paradox" effect at 10 Torr O_2 would likely have a consequence on the function of HbF_0 in vivo, unlike HbA_0. This effect would increase HbO_2 with increasing HbCO in the umbilical artery upon CO intoxication (lower curve in Figure 7a), making fetal blood more sensitive to CO intoxication than adult blood. Other linkage graphs can be constructed with the binding capacities of O_2 and CO, in order to show the effect of one ligand on the cooperativity of the other, i.e., linkage of higher order (Di Cera et al., 1988). Figure 8 shows how the O_2 binding capacity is drastically reduced by addition of CO in the case of HbF_0. The effect observed in the case of HbA_0 is practically identical. The reduction of the O_2 binding capacity due to an increase in the CO partial pressure is of biological relevance since the binding capacity is a thermodynamic measure of the efficiency of a macromolecule as a carrier.

In conclusion, the functional properties of HbF_0 are found to parallel those of HbA_0. This is indicated by (1) the negligible contribution of the triply ligated species, in any combination of O_2 and CO, to the ligation process of both Hbs, (2) the comparable O_2 and CO binding capacities for the two Hbs, and (3) the striking similarity between the extent of failure of the Haldane laws for both HbF_0 and HbA_0. This

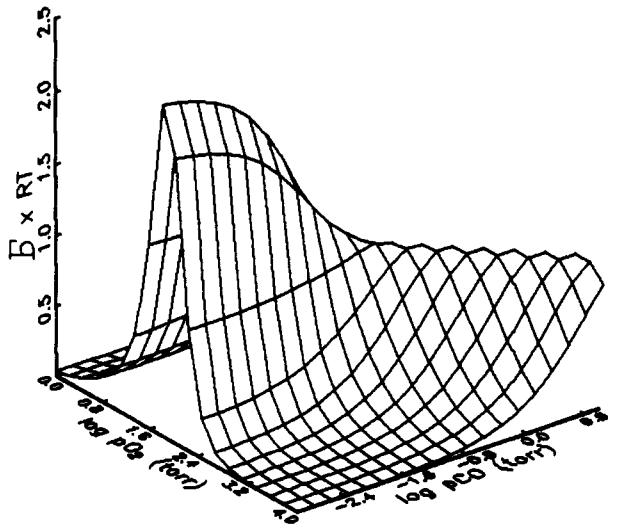

FIGURE 8: Linkage graph of the O_2 binding capacity of HbF_0 as a function of the O_2 and CO partial pressures. The graph was constructed with the values of the overall equilibrium constants listed in Table III. It shows the effect of the identical linkage on O_2 cooperativity, which is reduced upon addition of CO, as seen by the decrease of the maximum of the binding capacity.

suggests that the allosteric mechanism underlying the energetic changes of HbF_0 in its reaction with O_2 and CO must be similar to that of HbA_0 (Di Cera et al., 1987b). Nevertheless, the fundamental difference in the binding of O_2 and CO to the heme site, namely, the intrinsic tendancy of oxygen to bind in a bent geometry, while carbon monoxide prefers a linear geometry (Moffat et al., 1978), perhaps is the cause for the different response of cooperativity seen in both hemoglobins.

ACKNOWLEDGMENTS

We acknowledge many helpful discussions with Jeffries Wyman concerning the theory of identical linkage.

APPENDIX

This appendix summarizes the basic thermodynamic principles of the identical linkage theory and the concepts of relevance in the discussion of the O_2 and CO binding reactions to Hb. The principles apply to any system that can be described in terms of mass law binding phenomena (Wyman, 1984; Di Cera et al., 1988). Although they have been partly discussed elsewhere (Di Cera et al., 1987a), they are reconsidered here in expanded form for the sake of self-consistency of this paper.

Identical Linkage Theory. The thermodynamic approach to the partitioning of CO and O_2 to Hb is based on the principles of the "identical linkage" theory (Wyman, 1964). For a nondissociating tetrameric macromolecule the binding partition function, Ξ, can be expressed exactly in terms of four ligand binding sites as

$$\Xi(x) = 1 + \beta_1 x + \beta_2 x^2 + \beta_3 x^3 + \beta_4 x^4 \qquad \text{(A1)}$$

where x is the ligand activity and β_i is the overall equilibrium constant for the reaction $M + iX = MX_i$ (M denotes Hb). In the case of gaseous ligands like O_2 or CO, x is the ligand partial pressure. When both ligands are present, the general reaction scheme is

$$M + iX + jY = MX_iY_j \qquad \text{(A2)}$$

where X and Y denote O_2 and CO, respectively. The corresponding overall equilibrium constant for the species with i oxygens and j carbon monoxides bound is β_{ij} ($\beta_{00} = 1$). The linkage between CO and O_2 to Hb is "identical", in the sense defined by Wyman (1948), where both ligands bind to the same site (namely, the heme) and hence either ligand, once bound, excludes the binding of the other. In mathematical terms this means that the sum $i + j$ cannot exceed 4, the total number of heme sites. The binding partition function is given by

$$\Xi(x,y) = \sum_{i=0}^{4}\sum_{j=0}^{4-i}\beta_{ij}x^i y^j \qquad \text{(A3)}$$

where x and y are the O_2 and CO partial pressures, respectively. The allowed species are depicted in a triangular array as shown:

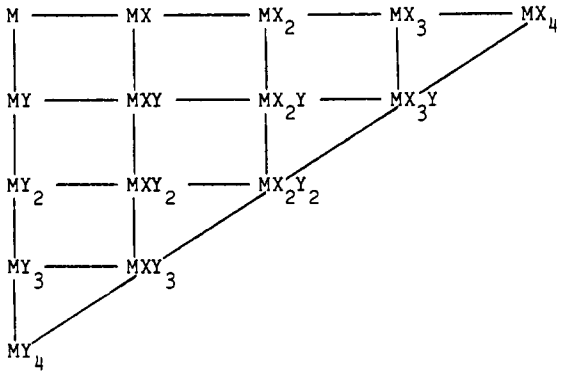

From eq A3 the number of moles of O_2 ($\bar{X}$) or CO ($\bar{Y}$) bound per mole of Hb is obtained by differentiation:

$$\bar{X} = \left(\frac{\partial \ln \Xi(x,y)}{\partial \ln x}\right)_{\ln y} \qquad \text{(A4a)}$$

$$\bar{Y} = \left(\frac{\partial \ln \Xi(x,y)}{\partial \ln y}\right)_{\ln x} \qquad \text{(A4b)}$$

From the relations above one verifies that $\bar{X} + \bar{Y} \leq 4$. Moreover, one can obtain a set of linkage relations such as (Wyman, 1948, 1964)

$$\left(\frac{\partial \bar{X}}{\partial \ln y}\right)_{\ln x} = \left(\frac{\partial \bar{Y}}{\partial \ln x}\right)_{\ln y} \qquad \text{(A5a)}$$

$$\left(\frac{\partial \bar{X}}{\partial \bar{Y}}\right)_{\ln x} = -\left(\frac{\partial \ln y}{\partial \ln x}\right)_{\bar{Y}} \qquad \text{(A5b)}$$

which can then be used in the construction of linkage graphs (Wyman, 1984). The treatment given above can easily be generalized to the case of an arbitrary number of binding sites.

The Binding Capacity. The linkage relations eq A5a and A5b involve heterotropic derivatives (Wyman, 1964) and are a measure of the interference of the two linked ligands. Homotropic cooperativity (Wyman, 1964), on the other hand, is a measure of the interactions involving only one type of ligand, e.g., O_2 or CO. The thermodynamic quantity that describes homotropic cooperativity is a partial derivative that gives the change in the number of ligands bound per mole of macromolecule ($\bar{X}$ or $\bar{Y}$) due to a change of the chemical potential of the ligand and has been termed the binding capacity B (Di Cera et al., 1988). In the case of the identical linkage of O_2 and CO one has

$$B_{X,\ln y} = \frac{1}{RT}\left(\frac{\partial \bar{X}}{\partial \ln x}\right)_{\ln y} \qquad \text{(A6a)}$$

$$B_{Y,\ln x} = \frac{1}{RT}\left(\frac{\partial \bar{Y}}{\partial \ln y}\right)_{\ln x} \qquad \text{(A6b)}$$

where R is the gas constant and T the absolute temperature. The binding capacity parallels the heat capacity in thermal

phenomena and is related to the Hill coefficient:

$$n_X = \frac{4RT}{\bar{X}(4 - \bar{X})}\mathbb{B}_{X,\ln y} \quad \text{(A7a)}$$

$$n_Y = \frac{4RT}{\bar{Y}(4 - \bar{Y})}\mathbb{B}_{Y,\ln x} \quad \text{(A7b)}$$

This quantity is of particular interest in the analysis of binding phenomena and has a close connection to differential binding measurements (Di Cera & Gill, 1988), as described in the text. It leads to a deeper understanding of the underlying reactions of the system and gives a quantitative measure of higher order linkage between two ligands.

The Haldane Laws. Haldane proposed two laws regarding the binding of CO and O_2 to Hb (Haldane & Smith, 1897). The first law says that when hemoglobin is exposed to a mixture of the two gases, the ratio of carbon monoxide $\bar{Y}$ to oxygen $\bar{X}$ molecules bound is proportional to the ratio of the partial pressures of the two gases ($y = p_{CO}$; $x = p_{O_2}$) according to a constant factor m, the partition coefficient; that is

$$\frac{\bar{Y}}{\bar{X}} = m\frac{y}{x} \quad \text{(A8)}$$

The second law is a consequence of the first one. It says that the total saturation $\bar{T} = \bar{Y} + \bar{X}$ is given by

$$\bar{T} = \bar{Y} + \bar{X} = f(x + my) \quad \text{(A9)}$$

and is a function of $x + my$ only. According to these laws the CO binding curve is expected to be parallel to the O_2 binding curve, the displacement of the two curves being given by the constant partition coefficient m. Accordingly, the partition coefficient surface derived from eq A8 by plotting m versus x and y (or their logarithm) must be flat. These predictions can be tested experimentally once the functions $\bar{Y}$ and $\bar{X}$ are known for any value of x and y.

Registry No. HbF_0, 72711-30-9; HbA_0, 54651-57-9; O_2, 7782-44-7; CO, 630-08-0.

References

Barcroft, J. (1928) *The Respiratory Function of the Blood*, Cambridge University Press, Cambridge.

Bunn, H. F., & Forget, B. G. (1986) in *Hemoglobin: Molecular, Genetic and Clinical Aspects*, W. B. Saunders Co., Philadelphia.

Castagnola, M., Caradonna, P., Salvi, M. F., & Rosetti, D. (1983) *J. Chromatogr. 272*, 51–65.

Castagnola, M., Caradonna, P., Cassiano, L., Degen, C., Lorenzin, F., Rosetti, D., & Salvi, M. L. (1984) *J. Chromatogr. 307*, 91–102.

Chu, A. H., Turner, B. W., & Ackers, G. K. (1984) *Biochemistry 23*, 604–617.

Dawes, G. S. (1965) *Handbook of Physiology*, Vol. II, pp 1313–1328, American Physiological Society, Washington, DC.

Di Cera, E., & Gill, S. J. (1988) *Biophys. Chem. 29*, 351–356.

Di Cera, E., Doyle, M. L., Connelly, P. R., & Gill, S. J. (1987a) *Biochemistry 26*, 6494–6502.

Di Cera, E., Robert, C. H., & Gill, S. J. (1987b) *Biochemistry 26*, 4003–4008.

Di Cera, E., Gill, S. J., & Wyman, J. (1988) *Proc. Natl. Acad. Sci. U.S.A. 85*, 449–452.

Dolman, D., & Gill, S. J. (1978) *Anal. Biochem. 87*, 127–134.

Douglas, C. G., Haldane, J. S., & Haldane, J. B. S. (1912) *J. Physiol. 44*, 275–304.

Doyle, M. L., Di Cera, E., & Gill, S. J. (1988) *Biochemistry 27*, 820–824.

Frier, J. A., & Perutz, M. F. (1977) *J. Mol. Biol. 112*, 107–112.

Gill, S. J., Di Cera, E., Doyle, M. L., Bishop, G. A., & Robert, C. H. (1987) *Biochemistry 26*, 3995–4002.

Gill, S. J., Connelly, P. R., Di Cera, E., & Robert, C. H. (1988) *Biophys. Chem. 30*, 133–141.

Haldane, J. S., & Smith, J. L. (1897) *J. Physiol. 22*, 231–258.

Hayashi, A., Suzuki, T., & Shin, M. (1973) *Biochim. Biophys. Acta 310*, 309–316.

Mills, F. C., Johnson, M. L., & Ackers, G. K. (1976) *Biochemistry 15*, 5350–5362.

Moffat, K., Deatherage, J. F., & Seybert, D. W. (1979) *Science 206*, 1035–1042.

Ratkowski, D. A. (1983) in *Non-linear Regression Modeling*, Marcel Dekker, New York.

Roughton, F. J. W. (1970) *Ann. N.Y. Acad. Sci. 174*, 177–188.

Schroeder, W. A., Shelton, J. R., Shelton, J. B., Cormick, J., & Jones, R. T. (1963) *Biochemistry 2*, 992–1008.

Spokane, R. B., Brill, R. V., & Gill, S. J. (1980) *Anal. Biochem. 109*, 137–145.

Wyman, J. (1948) *Adv. Protein Chem. 4*, 407–531.

Wyman, J. (1964) *Adv. Protein Chem. 19*, 233–286.

Wyman, J. (1984) *Q. Rev. Biophys. 17*, 453–488.

Wyman, J., Bishop, G. A., Richey, B., Spokane, R., & Gill, S. J. (1982) *Biopolymers 21*, 1735–1747.